Ashish Bhave*, Jash Joshi, Vaishnavi Yache, Stefan J. Rupitsch, Knut Moeller.

# Hyper-viscoelastic characterization of the urethra

https://doi.org/10.1515/cdbme-2024-2020

**Abstract:** Hyper-viscoelastic models have been used to characterize large strains coupled with viscosity. In this study, we aimed to model the urethral in-vivo biomechanics through a hyper-viscoelastic implementation. First, we used isotropic 2-parameter Demiray model for identification of urethral tube inflation after refining the values of quasistatic states. Attempting the approach by Holzapfel et. al., the average ratio of the elastic and dynamic modulus was computed to determine the stress contribution of the viscoelastic branches. The values of the parameters were determined after constraining a constant Energy dissipation (generalized maxwell) over range 1s to 100s. For the hyper-viscoelastic comparison implementation, it was observed that the goodness of fit criteria performs good for half of the samples (Adjusted $R^2$>0.95). In some samples, the model is limited to fit 'S' shape curves but still performed well. The above identification technique and the hyper-viscoelastic in-silico approaches show that our approach fares sufficiently for the creep response characterization of the urethra.

**Keywords:** Elastomers, Strain Sensing, Shape characterization, biomechanics, lumen, hyper-viscoelastic.

# 1 Introduction

A high compliant inflatable intra-luminal sensor-actuator system is currently under development at the research institutes of Furtwangen University for application within urethra/artery [1]. This system will be used to identify tissue biomechanics and geometrical properties in-vivo.

To enable realistic sensor-tissue simulations, it is first essential to individually characterize the tissue biomechanics. Hyperelastic models are widely used to characterize time-invariant (quasistatic level) tissue behaviour parameters defined by Delfino/Demiray [2]. More complex phenomenological models such as Holzapfel-Gasser-Ogden (HGO) [3], GOH model [4] etc. are available. Time varying effects (viscosity) have also been modelled as standard linear models ,as hyper-viscoelastic approaches from HGO [5], Fractional models [6] and others [7].

Urethra is a complex organ and has limited biomechanical studies carried out in a constrained environment and with certain approximations. It is the aim of this study to refine the biomechanical data using simple fitting methods and further apply a hyper-viscoelastic approach to capture both the hyperelastic and viscous effects of the urethra.

# 2 Methods

The dataset for urethral tube inflation was utilized Cunnane et.al. [8] In their experimental setup they applied a step pressure profile to the urethral tube (post elongating to its pre-excised axial prestretch) from 0 to 10 kPa in incremental steps of 1 kPa while each step was held for around 300s. This was performed to obtain the approximate static stretch levels of urethral tube. They later performed histological assessment on the samples to obtain the average thickness of tissues for each sample.

The method is divided into multiple steps for inflation:

2.1) Use the Pressure v/s Diametric extension profile to perform fitting by prediction of the ideal quasistatic states.

2.2) Use the predicted quasi-static values for each sample to identify the in-vivo hyperelastic model fit using 2 parameter Demiray model.

2.3) Calculate the average incremental modulus between the static and dynamic inflation profile from Cunnane Dataset [8] and use it to calculate the contribution of 3 generalized maxwell branches for constant Energy dissipation ( with procedure defined by HGO ) [5].

**Corresponding author: Ashish Bhave**: Institute of Technical Medicine, Furtwangen University, Jakob-Kienzle-Straße 17, Villingen-Schwenningen, Germany, e-mail: ashishbhave1993@gmail.com , ashish.bhave@hfu.eu
**Jash Joshi, Vaishnavi Yache:** Furtwangen University, Villingen-Schwenningen, Germany.
**Stefan J. Rupitsch:** Department of Microsystems Engineering, Georges-Köhler-Allee 106, Freiburg im Breisgau, Germany
**Knut Moeller:** Institute of Technical Medicine, Furtwangen University, Villingen-Schwenningen, Germany, knut.moeller@hfu.eu

2.4) Obtain the Pressure v/s Diametric extension data for the in-silico hyper-viscoelastic approach (Demiray+ generalized maxwell (HGO)) using the actual pressure profile for each sample. Comparing the goodness of fit for the experimental data and the in-silico simulations for the above curve.

## 2.1 Optimization

It is well known that tissues have a dynamic range of biomechanical properties. As time is generally a constraint to perform in-vivo experiments, methods can be utilized to optimize the data obtained. In the current case an exponential function was deployed to fit the parameters along with multistart algorithm to obtain a global minimum.

$$Ø = a_1 - (P_t * a_2) * e^{-t/a_3} \quad (1)$$

The 'a$_x$' are phenomenological parameters while $P_t$ is input vessel pressure at time 't'. $a_1$ parameter as standalone would provide the diameter 'Ø' when t=∞ (quasistatic equilibrium point), because the contribution of part with the exponent arrives to value of '0' . This equation is applied manually to each 50 second range for each pressure step at its end (when applied inflation pressure within urethral lumen was largely constant and changes in diameter were of relatively slower rate than the rest of the preceding part of step). The corresponding value for the diameter at the hypothetical t=∞ was computed for each incremental pressure step.

## 2.2 Demiray model fitting

Once the pressure v/s stretch values were obtained, a simple exponential based hyperelastic model was used to fit the 11 points (0:1:10 kPa) for each tubular sample. The equation is given by:

$$\left(A/_B\right) * \left(e^{B/_2*(\lambda_\theta^2+\lambda_r^2+\lambda_z^2-3)} - 1\right) \quad (2)$$

Where A is stress parameter and B defines the shape of the exponent. $\lambda_\theta$ $\lambda_r$ $\lambda_z$ are the principle stretch components that were obtained by simple calculations. A and B parameters were identified for each of the samples with assumption of tissue incompressibility and ideal cylindrical geometrical assumption.

## 2.3 Ratio of Static Dynamic inflation

The Cunnane et. al, dataset [8] provided the static and dynamic inflation curves. In this study we considered isovolumetric constraints and therefore the thickness of the cylindrical tube narrows as the tube inflates. We computed the average incremental modulus (over 0 to 10 kPa) for the static levels with the newly found diameters from step 2.1 and for the dynamic inflation data. The incremental modulus ($E_{inc}$) is a linear measure tissue's stiffness in response to an incremental increase in pressure [8]. The incremental modulus for thick cylindrical vessels is calculated as:

$$E_{\text{inc}} = \frac{\Delta P_I}{\Delta R_o}\left(\frac{2R_i^2 R_o}{R_o^2 - R_i^2}\right) + \left(\frac{2P_I R_o^2}{R_o^2 - R_i^2}\right) \quad (3)$$

Where $R_i$ is the internal radius, $R_o$ is the external radius and $P_I$ is the pressure at each increment. The incremental modulus was calculated for each sample for both static ($E_{stat}$) and dynamic ($E_{dyn}$) testing using the data provided by Cunnane et al. In principle, we could use in-vivo urethral saline volume and the external diameter measurements to approximate the thickness/inner radius, but we use the histological test data.

The viscoelastic behaviour was characterised by using one dimensional generalised maxwell model branch as formulated by Holzapfel et al. 2002 [5,9]. The relationship between Beta ($\beta_\alpha^\infty$) and $E_{inc}$ modulii for static ($E_{stat}$) and dynamic ($E_{dyn}$) tests is provided as follows:

$$\Sigma\beta_\alpha^\infty = \frac{E_{\text{dyn}}}{E_{\text{stat}}} - 1 \quad (4)$$

where $E_{dyn}$ / $E_{stat}$ is the ratio of the mean of incremental modulus of dynamic and static tensile testing range.

The two parameters that describe the viscoelastic process for a branch are $\beta_\alpha^\infty$ and $\tau_\alpha$. $\beta_\alpha^\infty$ is the dimensionless free energy factor (viscoelastic stress contribution) and $\tau_\alpha$ is the retardation time associated with the maxwell element branch in the model. These parameters contribute to the material response to time dependent stress [5]. In this we consider three maxwell elements in parallel to a free hyperelastic spring. Here we consider three viscoelastic branch and therefore $\Sigma\beta_\alpha^\infty = \beta_1^\infty + \beta_2^\infty + \beta_3^\infty$. We constrained the energy dissipation to be equal from 1s to 100s into 3 branches and consider $\tau_1$= 1s, $\tau_2$= 10s and $\tau_3$= 100s to encompass a wide spectrum where viscosity is prevalent. The determination of the $\beta_\alpha^\infty$ value was carried out by employing eq.3 for every individual sample.

## 2.4 Finite Element Method (FEM) vs experimental data

As noted previously, the step pressure profile used for vessel inflation undertaken for static analysis shows viscoelastic effects for each step. COMSOL (v6.2) was used to perform the forward modelling the chosen samples in-vivo inflation. The sample specific urethral sample geometry, in-vivo axial stretch was used to initialize the geometry. The identified Demiray hyperelastic model parameters A and B, the viscoelastic branch parameter $\beta_\alpha^\infty$ for each of the chosen time constants ($\tau_\alpha$ =1s, 10s and 100s) were used to initialize the mathematics of the model.

Incompressibility constraints were set, and penalty formulation was used to solve the FEM solutions. The 2D axisymmetric geometries were initialized by quadratic elements. The pressure was applied on the inner lumen of the vessel with the above pressure mentioned profile as input. The ideal boundary conditions related to the experimental setup were initiated. A mesh refinement study was undertaken to validate that the results stay within 0.5 percent error range.

We compared the simulated outer pressure v/s diameter to its corresponding experimental data. The estimation of goodness of fit for our non-linear fitting of the static profile fitting was performed using Adjusted coefficient of determination (Adjusted $R^2$).

# 3 Results and Discussion

The urethral tube is axially eccentric and has a varying thickness profile throughout its length. The spongy tissue surrounding the thin urethral tube gives pseudo compressibility to the structure due to the void vascular spaces which allow flow of blood in-vivo. These factors make the measurements sensitive to the site of measurements as well as other approximations. Owing to these approximations, unsuitable values were arrived for sample 2 and 4. The dataset for sample 8 did not provide the static analysis curves and therefore was excluded too.

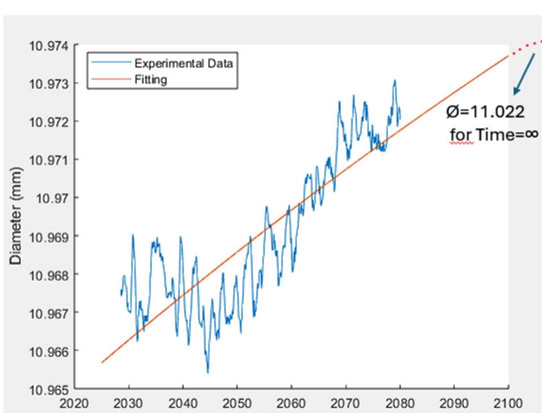


**Figure 1:** The example fitting of Diameter v/s Time for sample 1. Only the 10 *kPa* pressure step for period of 50*s* was considered. In case of standard approach, the quasistatic diameter would be assumed 10.97mm. But by fitting, the value arrived to is 11.022mm which is a 0.5% difference.

**Table 1:** The identified A and B Demiray parameters along with the value of the $\beta_\alpha^\infty$ branches for each sample. The adjusted $R^2$ value suggests good fitting for sample 1, 3 and 5 while not so good fitting for sample 7 and 9.

| *Sample* | $\tau_1,\tau_2,\tau_3$ *[s]* | $\beta_\alpha^\infty$ *[-]* | *A[kPa], B[-]* | *Adjusted $R^2$[-]* |
|---|---|---|---|---|
| 1 | 1, 10, 100 | 0.418 0.247 0.199 | 1.1057, 1.4016 | 0.959 |
| 3 | 1, 10, 100 | 0.901 0.533 0.431 | 0.864, 0.827 | 0.972 |
| 5 | 1, 10, 100 | 0.238 0.141 0.114 | 1.868 0.799 | 0.983 |
| 6 | 1, 10, 100 | 0.148 0.087 0.071 | 0.872, 0.047 | 0.909 |
| 7 | 1, 10, 100 | 0.037 0.022 0.017 | 0.254, 3.226 | 0.814 |
| 9 | 1, 10, 100 | 0.565 0.336 0.272 | 0.424, 0.105 | 0.848 |

A refinement as detailed in 2.1 was applied to the remaining samples and an example of fitting with sample 1 for 10 *kPa* step for its 50s duration is shown in Figure 1. In the approximate case, the static diameter would have been 10.97*mm* but due to the fitting, the predicted value is 11.02*mm*. In the refined approach predicted values were seen to increase by 0.5-5 percent of the experimental outer diameter stretches, with more deviation in the initial of pressure steps. If the diametric stretches in the lumen of the vessels were computed, the effects were significantly larger. We can infer from the fit values that the experimental approach underestimates the elasticity by a few percentages for the outer diameter with more deviation in the initial pressure region. The identified values of A and B of the Demiray model in many cases shows

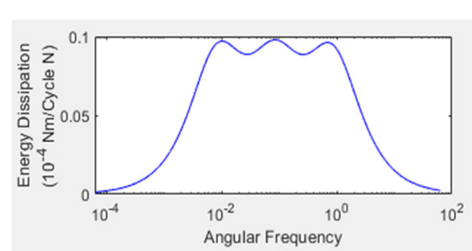


**Figure 2:** The Energy dissipation is constant across angular frequency from $10^{-2}$ ($\tau$ =100s) until $10^{0}$ ($\tau$=1s).

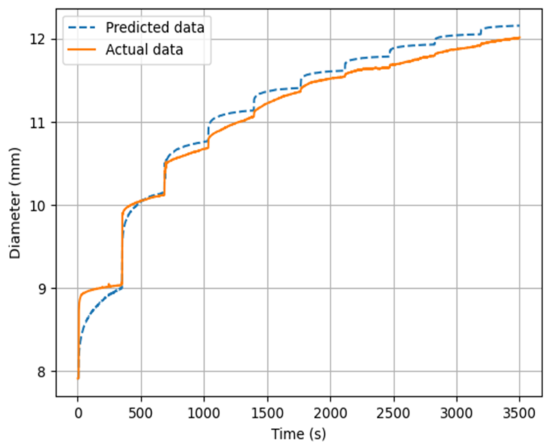


**Figure 3:** FEM procedure outputs for sample 3 using partial fitting and assumptions shows a good comparable output (Adjusted R2>0.95) using the hyper-viscoelastic approach. The experimental data suggests the viscous behaviour in tissues is dynamic and finetuning of energy dissipation can show better results.

significant deviation of more than 15-20% for the refined dataset in comparison to standard assumed levels (unrefined dataset) [in publication, Bhave et al]. Smaller 'A' parameter will have a physiological correlation that the elastin content is more as percentage within tissues, while smaller 'B' values can be interpreted that the collagen stiffening effects are triggered later and tissue is more compliant.

We can observe from the Figure 2 that the Energy Dissipation is constrained and remains approximately constant for $\tau_\alpha = 1s$ till $100s$ (Angular frequency $10^{-2}$ *Hz* till $10^{0}$ *Hz*) The end result comparison plots are largely due to the effect of: 1) A and B Demiray parameters, 2) Assumption of average dynamic:static incremental modulus ratio and 3) Assumption of constant Energy dissipation between range of 1s to 100s. The samples 1,3,5 show good fitting characteristics as evident from 'Adjusted $R^2$' values seen in table 1. It has been observed that the hyperelastic behaviour of tissues is 'S' shaped in certain cases. The simplicity of the Demiray model due to its 2 parameters is also its limitation as it cannot accurately replicate certain non-linear urethral biomechanics (samples 6 ,7 and 9). In Figure 3, we observe how the FEM outputs fare in comparison to the experimental data. The Demiray model is limited by the curvature it can obtain; performs good (see Table 1) in over half of samples.

The hyperviscoelastic model approach by shows good capacity to model the dissipation in the viscous branches to be fine-tuned according to the application. With more experimental data w.r.t dynamic testing, the energy dissipation for each viscoelastic branch can be computed.

# 4 Conclusion

From a clinical perspective, accurate characterization of tissue biomechanics during surgery using predictive techniques can aid the surgeon to make informed decisions and therefore less chance of errors.

Based on the important points from the current study, it is intended to further the simulations with 3D setup and anisotropic characterization of vessels to obtain more realistic measurements. In future scope we aim to attempt at obtaining simplified analytical solutions for tissue hyperviscoelasticity.


### Author Statement

This research was partly supported by the German Federal Ministry of Research and Education (BMBF) under grant no. 2522FSB903-PerFluid (ERA PerMed) and under grant no. 13FH066KX2 (DiaKatPlus/FH-Kooperativ)


## References


[1] Sittkus B, Zhu R, Mescheder U. Flexible piezoresistive PDMS metal-thin-film sensor-concept for stiffness evaluation of soft tissues. In: 2019 IEEE International Conference 7/2019: 1–3.

[2] Demiray H. A note on the elasticity of soft biological tissues. Journal of biomechanics 1972; 5: 309–311.

[3] A New Constitutive Framework for Arterial Wall Mechanics and a Comparative Study of Material Models.

[4] Gasser TC, Ogden RW, Holzapfel GA. Hyperelastic modelling of arterial layers with distributed collagen fibre orientations. Journal of the Royal Society, Interface 2006; 3:15-35.

[5] Holzapfel GA. ON LARGE STRAIN VISCOELASTICITY: CONTINUUM FORMULATION AND FINITE ELEMENT APPLICATIONS TO ELASTOMERIC STRUCTURES. Int. J. Numer. Meth. Engng. 1996; 39: 3903–3926.

[6] Bagley RL, Torvik PJ. Fractional calculus in the transient analysis of viscoelastically damped structures. AIAA Journal 1985; 23: 918–925.

[7] Shitikova MV, Krusser AI. Models of Viscoelastic Materials: A Review on Historical Development and Formulation. In: Giorgio I, Placidi L, Barchiesi E, Abali BE, Altenbach H, editors. Theoretical Analyses, Computations, and Experiments of Multiscale Materials. Cham: Springer International Publishing; 2022: 285–326.

[8] Cunnane EM, Davis NF, Cunnane CV, et al. Mechanical, compositional and morphological characterisation of the human male urethra for the development of a biomimetic tissue engineered urethral scaffold. Biomaterials 2021; 269: 120651.

[9] Holzapfel GA, Gasser TC, Stadler M. A structural model for the viscoelastic behavior of arterial walls: Continuum formulation and finite element analysis. European Journal of Mechanics - A/Solids 2002; 21: 441–463.